Peer-reviewed version available at *Galaxies* **2018**, *6*, 136; doi:10.3390/galaxies6040136

Article

DETECTION OF PERIODIC RADIO SIGNAL FROM THE BLAZAR J1043+2408

Gopal Bhatta [1,†,‡] *

[1] Astronomical Observatory, Jagiellonian University, ul. Orla 171, 30-244 Kraków, Poland; gopalbhatta716@gmail.com

* Correspondence: gopalbhatta716@gmail.com; Tel.: +x-xxx-xxx-xxxx

Abstract: Search for periodic signals from blazars has become widely discussed topic in recent years. This is because periodic signals bear imprints of the processes occurring near the innermost regions of blazars which are mostly inaccessible to our direct view. Such signals provide insights into various aspect of blazar studies including disk-jet connection, magnetic field configuration and, more importantly, strong gravity near the supermassive black holes and release of gravitational waves from the binary supermassvie black hole systems. In this work, we report detection of a periodic signal in the radio light curves of the blazar J1043+2408 spanning ∼10.5 years. We performed multiple methods of time series analysis, namely, epoch folding, Lomb-Scargle periodogram, and discrete auto-correlation function. All three methods consistently reveal a repeating signal with a periodicity of ∼ 563 days. To robustly account for the red-noise processes usually dominant in the blazar variability and other possible artifacts, a large number of Monte Carlo simulations were performed. This allowed us to estimate a high significance (99.9% local and 99.4% global) against possible spurious detection. As possible explanations, we discuss a number of scenarios including binary supermassive black hole system, Lense-Thirring precession, and jet swing and precession.

Keywords: Supermassive black holes: non-thermal radiation; active galactic nuclei: BL Lacertae objects: individual: J1043+2408; galaxies: jets; method: time series analysis

1. Introduction

Blazars, a class of radio-loud active galactic nuclei (AGN), are the most powerful sources in the universe. The sources have relativistic jets beamed upon us that shine brightly in non-thermal emission covering a wide electromagnetic spectrum - from radio to most energetic γ-rays. As the jets shoots out matter with high speeds along the line of sight, relativistic effects become dominant resulting in the Doppler boosted emission that is highly variable over the entire electromagnetic spectrum [1]. The broadband spectral energy distribution (SED) of blazars can often be identified with the double-peaked feature in the frequency-flux plane. The lower peak, usually found between the radio and the X-ray, arises as a result of the synchrotron emission by the energetic particles accelerating in the jet magnetic field; whereas the high frequency peak, mostly lying between UV to γ-ray, is believed to the result of the inverse-Compton scattering of the soft seed photons by high-energy particles [see 2,6, and the reference therein].

Blazars consist of two types of sources: flat-spectrum radio quasars (FSRQ) and BL Lacertae (BL Lac) objects. FSQRs are the more powerful sources which show emission lines over the continuum and have the synchrotron peak in the lower part of the spectrum; whereas BL Lac objects are less powerful ones which show weak or no emission lines and have synchrotron peak in the higher part of the spectrum. BL Lac sources represent an extreme class of sources with maximum synchrotron and inverse-Compton emission output ranging from hard X-rays to TeV emission. The sources do not possess strong circum-nuclear photon fields and are believed to accrete at relatively low rates [see 2, and references therein].

Preprints (www.preprints.org) | NOT PEER-REVIEWED | Posted: 17 September 2018 doi:10.20944/preprints201809.0283.v1

Peer-reviewed version available at Galaxies 2018, 6, 136; doi:10.3390/galaxies6040136

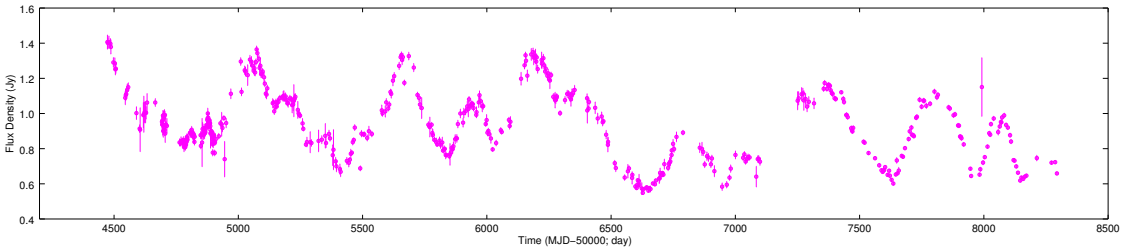

Figure 1. $\sim$ 10.5 years long 15 GHz observations of the blazar J1043+2408 from OVRO

Blazars display variability in a wide range of temporal frequencies - equivalently, on diverge timescales ranging from a few minutes to decades. The statistical nature of such variability can fairly be represented by a featureless power-law power spectral density (PSD) [see in this context 3,4, and references therein]. However, signatures of quasi-periodic oscillations (QPO) in the multi-frequency blazar light curves, including radio, optical, X-ray and γ-ray, have been found. The timescales of the reported periodicity range from a few hours to a few years [see 5–8, for QPOs in blazars].

In particular, at radio frequencies QPO on diverse timescales have been recorded in a number of blazars: In BL Lac source PKS 0219-164 a strong signal of QPO with 270 d period, along with possible low-frequency harmonics, was detected [6]. Similarly, in BL Lac source AO 0235, QPOs with periods ranging from about one year up to several years have been reported ([9,10]. Also, FSRQ J1359+ 4011 was reported to exhibit persistent $\sim$ 150 day periodic modulation in the 15 GHz observations [11]. In addition, several other blazar sources were found to show QPOs in the radio frequencies, e.g., FSRQ PKS 1510-089 [12], blazar NRAO 530 [13], and FSRQ PKS 1156+295 [14–16].

BL Lac J1043+2408 (RA=10h 43m 09.0s, Dec= +24d 08m 35s, and z = 0.563446; [17]) has been detected across diverge electromagnetic frequencies using most of the currently available instruments. The source is cataloged in Fermi/LAT as 3FGL J1043.1+2407 [18], and in Soft X-ray (0.1-2.4 keV) it is frequently observed by ROSAT [19]. During The Micro-Arcsecond Scintillation-Induced Variability Survey III, its optical (R-band) brightness was recorded to be 16.84 magnitudes [20]. The blazar is being regularly monitored in the 15-GHz radio band by the 40-m telescope of the Owens Valley Radio Observatory (OVRO) since 2008.

In this paper, we analyze the long term ($\sim$ 10.5 years) radio observations of the blazar J1043+2408 and report the detection of 563 d periodicity in the light curve. In section 2 we discuss data acquisition and in section 3 we present the time series analysis of the light curve using the epoch-folding Lomb-Scargle periodogram (LSP) and discrete auto-correlation function. We report presence of a statistically significant periodic oscillations in the flux with a characteristic timescale of 563 days. In addition, using Monte Carlo simulations, the significance of the detection over underlying red-noise processes was found to be $>$ 99%. In section 4, we discussion various possible scenarios that can lead to the observed periodicity, and finally we summarize our conclusion in section 5.

2. Data Acquisition

The 15 GHz radio observations of the source J1043+2408 were obtained from Owens Valley Radio Observatory (OVRO; [21]). We analyzed the observations, with an average sampling of a week, from the year 2008-01-08 to 2018-07-08 (equivalently, from MJD 54473 to 58307), spanning 3820 days ($\sim$ 10.5 years) .

3. Analysis and Results

The 15 GHz band light curve of the blazar J1043+2408 from the last decade is presented in Figure 1. In the figure, it can be clearly seen that not only the source displays long-term variability but it also shows a periodic flux modulation such that in each cycle the flux nearly doubles between minimum

Preprints (www.preprints.org) | NOT PEER-REVIEWED | Posted: 17 September 2018 doi:10.20944/preprints201809.0283.v1

Peer-reviewed version available at Galaxies 2018, 6, 136; doi:10.3390/galaxies6040136

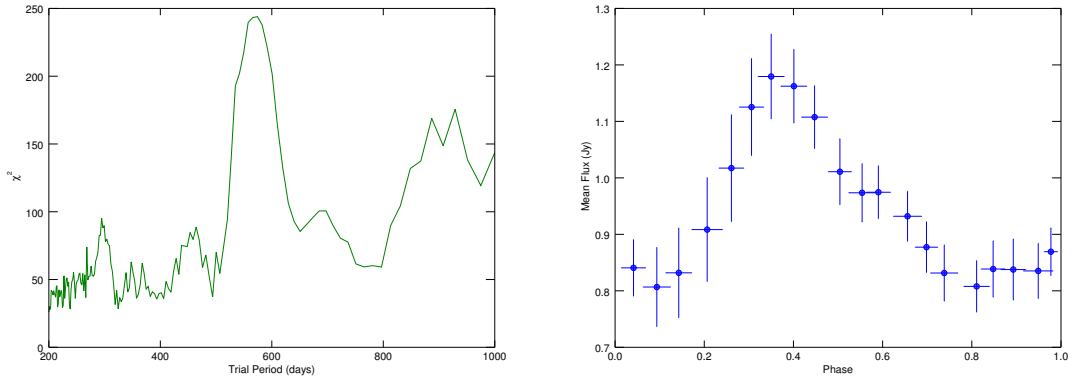

Figure 2. Epoch folding of the radio light curve of the blazar J1043+2408. Left panel: χ^2 values for the trial periods between 200 and 1000 days. Right panel: pulse profile of the periodic component for the timescale of 563 days representing maximum χ^2 value.

and maximum. To quantify the observed long-term variability, we estimated a fractional variability [22,23] of 20.29 ± 0.63 % , indicating a moderate variability over the period.

3.1. Periodicity Search:

To carry out the periodicity search analysis from different approaches, it was performed using three well known methods of time-series analysis: epoch folding, Lomb-Scargle periodogram and discrete auto-correlation function. The methods, analyses and the results are discussed in detail below.

3.1.1. Epoch folding

Epoch folding, a widely discussed method of time series analysis, was first worked out by Leahy et al. (1983) [24] and later improved by a number of authors [e.g. 25,26]. Unlike traditional discrete Fourier periodogram, which expects the periodic component to be of the sinusoidal shape, the method is less sensitive to the modulating shape of the periodic components. Also, this method is largely unaffected by the irregularity in the sampling of the observations and therefore well suited for the periodic search in the data with gaps. In this method, a time series of N data points are folded on a trial period and in a phase bin with M points. Then, a quantity χ^2 is expressed as

$$\chi^2 = \sum_{i=1}^{M} \frac{(x_i - \bar{x})^2}{\sigma_i^2}, \tag{1}$$

is estimated. For a Gaussian noise with a spread represented by standard deviation (σ_i), we find $\chi^2 \sim M$; however in case of the observations containing periodic signals, it takes a value which is significantly different (or the maximum) from the average value [for details refer to 28]. The method has been frequently tested for the periodicity search in blazar light curves e.g., [27].

We computed χ^2 values of the source light curve for the trial periods between 200 and 1000 days using a time step of 14 days. The pulse profiles corresponding to these trial periods were generated and, subsequently, tested for χ^2 constancy using Equation 1. The left panel of Figure 2 presents the distribution of the χ^2 values over the trial periods considered. The maximum χ^2 deviation seen at $\sim$ 563 days, represents the most probable period. The right panel of Figure 2 shows the pulse profile corresponding to the period. The observed period is further tested by using the following methods.

Preprints (www.preprints.org) | NOT PEER-REVIEWED | Posted: 17 September 2018 doi:10.20944/preprints201809.0283.v1

Peer-reviewed version available at Galaxies 2018, 6, 136; doi:10.3390/galaxies6040136

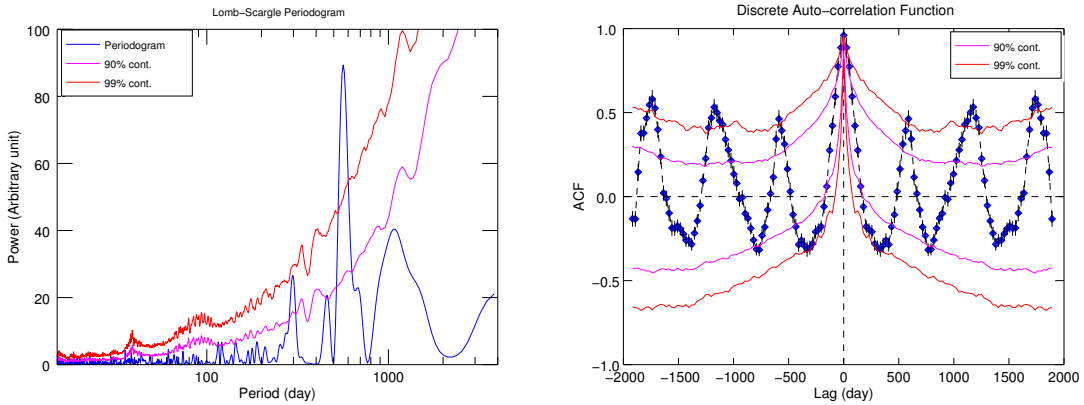

Figure 3. Lomb-Scargle periodogram (left panel) and discrete auto-correlation function (right panel) of the $\sim$ 10.5 years long 15 GHz observations of the blazar J1043+2408. The magenta and the red curves represent the 90 and 99% significance levels, respectively, from MC simulations.

3.1.2. Lomb-Scargle Periodogram

Lomb-Scargle Periodogram [LSP; 29,30] is one of the most popular methods of time series mostly suited for irregular sampling as in astronomical observations [see 4,6,7]. The method as a form of least-square fitting of the sinusoidal waves to the data is less sensitive to the gaps in the data when compared to the traditional discrete Fourier transform (DFT). Consequently, the fitting process enhances the periodogram features (or peaks) that can possibly represent periodic signals in the light curve. The LSP of the source light curve was computed for the minimum and maximum frequencies of, $1/f_{min} = 3820$ d, and f_{max}=1/14 d, respectively. The total number of periodogram frequencies were evaluated using

$$N_{eval} = n_0 T f_{max}, \tag{2}$$

where $n_0 = 10$, and $T = 3820$ days represents the total length of the observations [see 31]. The Lomb-Scargle periodogram of the $\sim$10.5 years long OVRO light curve of the blazar J1043+2408 is presented in Figure 3. It can be seen that in the periodogram a distinct peak stands out around the timescale of 563 ± 36 days suggesting presence of a strong periodic signal at the timescale. The uncertainties in the period are estimated by taking the half-width at the half-maximum (HWHM) of the peaks [see 6,7]. The result is in consistent with the previous finding by the epoch folding method.

3.1.3. Discrete auto cross-correlation Function

To further confirm the presence of the above periodic timescale using different method, we performed the discrete correlation function analysis as described in [32]. The method has been mostly applied to investigate cross-correlation between two time series with uneven spacing [see 2–4,23]. With only one light curve, the method becomes discrete auto-correlation function (ACF), which can be exploited to reveal the periodic signals in a light curve. The ACF, although related to PSD in frequency space, is computed in time domain and therefore it is free of the sampling effects such as windowing and aliasing. The method has been frequently employed in the periodicity search in blazar light curves [e.g. 2,33]. The discrete ACF of the radio light curve of the blazar is presented in right panel of Figure 3 which clearly reveals presence of the periodic behavior represented by the ACF peaks recurring after a lag interval of $\sim$ 563 days.

3.1.4. Significance Estimation and Monte Carlo Simulation

After we have employed three different methods to detect the periodicity in the light curve, it should be pointed out that, in general, the statistical properties of blazar light curves can be characterized as red-noise processes that can potentially mimic a transient periodic behavior, especially in the low-frequency domain [see 3,6,34, for the discussion]. In addition, spurious peaks might arise owing to other sampling effects including discrete sampling, finite observation period and uneven sampling of the light curve. Therefore, it is important to make consideration of these effects in the significance estimation against spurious detection. To address the issue, we followed the power response method [PSRESP; 35], a method extensively used in the characterization of the AGN power spectrum density [see 2,4,6,7, and references therein]. First the source periodogram was modeled with a PSD of power-law form, i.e., $P(\nu) \propto \nu^{-\beta} + C$; where ν, β, and C represent temporal frequency, spectral slope and Poisson noise level, respectively. Then, a large number of (typically 10000) light curves were simulated following the Monte Carlo (MC) method described in [36]. Subsequently, the simulated light curves were re-sampled to match the sampling of the source light curve. Now to estimate the significance of the periodic feature seen in the LSP, the LSP distribution of the simulated light curves was analyzed [for further details see 2,4,6,7]. The local significance of the observed periodic feature at the period of ∼563 d turned out to be ∼99.4%. Furthermore, since we do not possess a priori knowledge of the period at which the significant peak is likely to occur, the global significance, the fraction of the simulated LSP powers at any period below the observed power at the period of our interest, was also estimate [see 6]. We evaluated the global significance of the LSP peak at the period ∼563 day to be 99.6%. Similarly, the local 90% and 99% LSP significance contours are represented by the magenta and the red curves, respectively, in the left panel Figure 3. In similar way, we used the distribution of the simulated ACFs to estimate the local 90% and 99% significance contours shown by the magenta and the red curves, respectively, in the auto-correlation function shown in the right panel of Figure 3. The observed high significances imply a low probability of spurious detections and therefore suggests that the signal, intrinsic to the source light curve, should have a physical origin.

4. Discussion

Study of periodic oscillations in blazar could be a novel method to investigate the processes occurring at the innermost regions of the active central engines. The studies could provide important insights into a number of blazar aspects including strong gravity environment around fast spinning supermassive black holes (SMBH), magnetic filed configuration near the accretion disk, disk-jet connection and release of gravitational waves (GW) from the binary supermassvie black hole systems. There could be a number of processes that can explain the observed periodic flux modulations. Below we discuss some of them.

First, for the observed period (P_{obs}) of 563 days, the corresponding period in the source rest frame (P) at $z = 0.563$ is 360.10 days, as estimated using $P = P_{obs}/(1+z)$. From the obtained period, we can the estimate radius of Keplerian orbits around the central black hole as given by

$$\tau_k = 0.36 \left(\frac{M}{10^9 M_\odot}\right) \left(\frac{a}{r_g}\right)^{3/2} \text{days}, \tag{3}$$

where a is the length of the semi-major axis of the elliptic orbits. For a black hole of mass of $10^9 M_\odot$ the radius of the Keplerian orbit is estimated as $\sim 100\, r_g$, equivalently, ∼0.005 parsecs. Now this result can be interpreted in terms of binary supermassvie black hole system [e.g., 37], which potentially can explain presence of year-like periodic timescales in AGN [see for a review 38]. For the binary mass ratios in the rage 0.1–0.01, the orbital decay timescale in the GW-driven regime can be computed as

$$\tau_{insp} = 3.05 \times 10^{-6} \left(\frac{M}{10^9 M_\odot}\right)^{-3} \left(\frac{a}{r_g}\right)^{4} \text{years}, \tag{4}$$

Preprints (www.preprints.org) | NOT PEER-REVIEWED | Posted: 17 September 2018 doi:10.20944/preprints201809.0283.v1

Peer-reviewed version available at Galaxies 2018, 6, 136; doi:10.3390/galaxies6040136

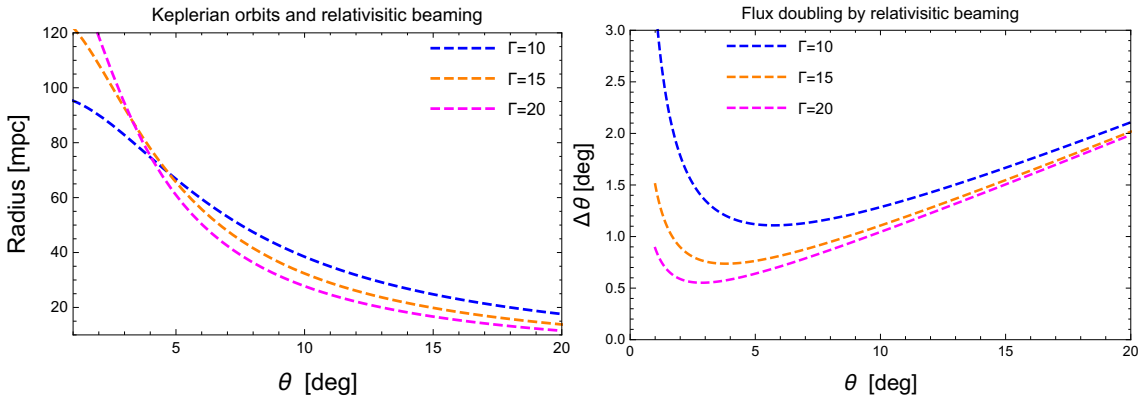

Figure 4. Left panel: Change in the radii (in milli-parsecs; mpc) of the circular orbits around the black hole of mass of $10^9 M_\odot$ corresponding to the 563 d periodicity exhibited by the emission region in the blazar jet as viewing angle changes for $\Gamma = 10, 15$, and 20. Right panel: The change in the viewing angle as a function of viewing angle for $\Gamma = 10, 15$, and 20 required to double the apparent flux, keeping intrinsic flux constant, via relativistic beaming. A radio spectral index α=0.6, typical of blazars, is used here.

[see 39]; the timescale is turns out to be less than a thousand years. Indeed, existence of binary SMBH is consistent with the prediction by hierarchical galaxy formation models. As a matter of fact, the closest binary SMBH so far detected lies the sub-parsec separation (0.35 pc; [40]) in Mrk 533, a Seyfert type 2 AGN. Therefore if the above periodicity is resulted from such a system, we should expect that the system go gravitational collapse within a few centuries accompanied with the emission of gravitational waves of the frequency $\sim 10^{-2}$ μHz. However, the probability of observing such a close (milliparsec) system of binary SMBH might be too small [see 41]. But on the other hand if the periodic changes are associated the relativistic motion of the emission regions along the helical path of the magnetized jets [e.g., 42,43], the periodic timescales can be longer by a factor of Doppler factor, $\delta = (\Gamma\,(1 - \beta cos\theta))^{-1}$, where for emission regions moving with the speed $\beta = v/c$ along the blazar jet making angle θ to the line of sight, the bulk Lorentz factor can be written as, $\Gamma = 1/\sqrt{1-\beta^2}$. Consequently, if we further assume that the periodic jet modulations are, in fact, induced in the SMBH system, the Keplerian orbit of the secondary black hole can lie farther away to a distance of a few sub-parsecs. The separation incidentally represents a relatively stable configuration in the evolution of binary SMBH systems [see 44]. Left panel of Figure 4 shows the radii of the Keperian circular orbits of the possible secondary black hole corresponding to periodic modulations propagating with three different bulk Lorentz factors, $\Gamma = 10, 15$, and 20, along the blazar jet that is viewed within 20^o.

Alternatively, periodic changes in the viewing angle can also lead to the observed periodic behavior. In blazar jets, when the emission regions move with a high bulk Lorentz factor, Γ, along the trajectory making an angle with the line of sight, because of the Doppler boosting, the rest frame flux (F'_ν) and observed flux (F_ν) are related through the equations

$$F_\nu = \delta^{3+\alpha} F'_{\nu'} \quad \text{and} \quad \delta(t) = 1/\Gamma\,(1 - \beta cos\theta(t)) \tag{5}$$

[see 6, and references therein]. For blazars having typical radio spectral index ($\alpha_R = 0.6$), the amount of jet swing required to double the observed flux, while keeping the flux in the source rest frame constant, for various jet angles and three bulk Lorentz factors $\Gamma = 10,\ 15$ and 20, is displayed in Figure 4. As the figure shows, for a typical jet angle of 10^o, a slight change in the viewing angle e.g., $\sim 1^o$, is sufficient to double the observed brightness.

Periodic behaviors in astronomical systems are also frequently interpreted in the context of the Lense-Thirring precession of accretion disks [e.g. 45,46]. In General Relativistic treatment of a massive

rotating objects, the nearby inertial frames are distorted by frame-dragging resulting in the nodal precession of the tilted orbits. Lense-Thirring precession timescale is proportional to the distance cubed and also to the mass of the central black hole so that the timescale can be expressed as

$$\tau_{LT} = 0.18 \left(\frac{1}{a}\right) \left(\frac{M}{10^9 M_\odot}\right) \left(\frac{r}{r_g}\right)^3 \text{days}. \quad (6)$$

For a maximally spinning ($a = 0.9$) central black hole mass with a mass $10^9 M_\odot$, a time scale of 360 days places the emission region around $\sim 12\, r_g$. The periodic oscillations could be the result of the jet precession due to such warped accretion disks. However, such a periodic timescale would be thousands of years, hence may not be relevant here [47,48].

In another likely scenario, the detected QPO with a periodicity of ~ 563 days could be explained in the context of highly magnetized jets and rotating magnetic field. In radio-loud AGNs the magnetic flux accumulation in the accretion disk can result in the formation of so-called *magnetically choked accretion flow*. In that case, owing to sudden change in the density and the magnetic flux, disk instabilities e.g., the Rayleigh-Taylor and Kelvin-Helmholtz instabilities, are set up; this in turn can induce QPOs at the disk-magnetosphere interface [49,50]. Similar QPOs have been observed in the recent magneto-hydrodynamical simulations of the large scale jets [51]. The periodic timescale of these QPOs could range from a few days to a few years depending upon the black hole mass and the spin parameter.

5. Conclusion

The long term ($\sim$10.5 years) radio (15 GHz) observations of the blazar J1043+2408 was analyzed for possible periodicity using three methods widely used in the astronomical time series: epoch folding, Lomb-Scargle periodogram and auto-correlation function. The study revealed a strong periodic signal with a ~ 563 day periodicity. A large number of Monte Carlo simulation of the light curves were used to establish a high significance ($> 99\%$) of the signal against possible spurious detection. We conclude that while other above discussed scenarios can not be completely rule out, periodic perturbation in binary SMBH system seems a more plausible mechanism at the root of the observed periodic radio signal.

Acknowledgments: We acknowledge the financial support by the Polish National Science Centre through the grant UMO-2017/26/D/ST9/01178. This research has made use of data from the OVRO 40-m monitoring program (Richards, J. L. et al. 2011, ApJS, 194, 29) which is supported in part by NASA grants NNX08AW31G, NNX11A043G, and NNX14AQ89G and NSF grants AST-0808050 and AST-1109911.

Conflicts of Interest: The authors declare no conflict of interest

Abbreviations

The following abbreviations are used in this manuscript:

AGN	Active Galactic Nuclei
ACF	Auto-correlation function
BL Lac	BL Lacertae object
FSRQ	Flat Spectrum Radio Quasar
LSP	Lomb-Scargle Periodogram
MC	Monte Carlo
OVRO	Owens Valley Radio Observatory
PSD	Power spectral density
QPO	Quasi-periodic oscillation
SMBH	Supermassive black hole

References

1. Meier, D. L. , Black Hole Astrophysics: The Engine Paradigm, Springer, Verlag Berlin Heidelberg, **2012**
2. Bhatta, G., et al. Hard X-ray Properties of NuSTAR Blazars, *A&A*, **2018**, in press (arXiv:1805.06957)
3. Bhatta, G., Stawarz, L., Markowitz, A., et al. Signatures of the disk-jet coupling in the Broad-line Radio Quasar 4C+74.26, *ApJ*, **2018**, in press (arXiv:1805.06957)
4. Bhatta, G., Stawarz, L., Ostrowski, M., et al. Multifrequency Photo-polarimetric WEBT Observation Campaign on the Blazar S5 0716+714: Source Microvariability and Search for Characteristic Timescales *ApJ* **2016**, 831, 92B
5. Gupta, A. Multi-Wavelength Intra-Day Variability and Quasi-Periodic Oscillation in Blazars *Galaxies*,, **2018**, 6, 1
6. Bhatta, G., Radio and γ-Ray Variability in the BL Lac PKS 0219 − 164: Detection of Quasi-periodic Oscillations in the Radio Light Curve, *ApJ*, **2017**, 487, 7B
7. Bhatta, G., Zola S., Stawarz, L., et al. Detection of Possible Quasi-periodic Oscillations in the Long-term Optical Light Curve of the BL Lac Object OJ 287, *ApJ*, **2016**, 832, 47
8. Zola, S., Valtonen, M., Bhatta, G., et al. A Search for QPOs in the Blazar OJ287: Preliminary Results from the 2015/2016 Observing Campaign *Galaxies*, **2016**, 4, 41
9. Liu, F. K., Zhao, G., & Wu, X.-B. Harmonic QPOs and Thick Accretion Disk Oscillations in the BL Lacertae Object AO 0235+164 *ApJ*, **2006**, 650, 749
10. Raiteri, C. M., Villata, M., Aller, H. D., et al. Optical and radio variability of the BL Lacertae object AO 0235+16: A possible 5-6 year periodicity *A&A*, **2001**, 377, 396
11. King, O. G., Hovatta, T., Max-Moerbeck, W., et al. A quasi-periodic oscillation in the blazar J1359+4011 *MNRAS*, **2013**, 436, L114
12. Xie, G. Z., Yi, T. F., Li, H. Z., Zhou, S. B., & Chen, L. E. *AJ*, **2008**, 135, 2212
13. An, T., Baan, W. A., Wang, J.-Y., Wang, Y., & Hong, X.-Y. *MNRAS*, **2013**, 434, 3487
14. Wang, J.-Y., An, T., Baan, W. A., & Lu, X.-L. Periodic radio variabilities of the blazar 1156+295: harmonic oscillations *MNRAS*, **2014**, 443, 58
15. Hovatta, T., Tornikoski, M., Lainela, M., et al. Statistical analyses of long-term variability of AGN at high radio frequencies *A&A*, **2007**, 469, 899
16. Hovatta, T., Lehto, H. J., & Tornikoski, M. Wavelet analysis of a large sample of AGN at high radio frequencies *A&A*, **2008**, 488, 897
17. Hewett, P. C., & Wild, V. Improved redshifts for SDSS quasar spectra *MNRAS*, **2010**, 405, 2302
18. Acero, F., Ackermann, M., Ajello, M., et al. Fermi Large Area Telescope Third Source Catalog *ApJS*, **2015**, 218, 23
19. Massaro, E., Giommi, P., Leto, C., et al. Roma-BZCAT: a multifrequency catalogue of blazars *A&A*, **2009**, 495, 691
20. Pursimo, T., Ojha, R., Jauncey, D. L., et al. The Micro-Arcsecond Scintillation-Induced Variability (MASIV) Survey. III. Optical Identifications and New Redshifts *ApJ*, **2013**, 767, 14
21. Richards, J. L., Max-Moerbeck, W., Pavlidou, V., et al. Blazars in the Fermi Era: The OVRO 40 m Telescope Monitoring Program, *ApJS*, **2011**, 194, 29
22. Vaughan, S., Edelson, R., Warwick, R. S., & Uttley, P. On characterizing the variability properties of X-ray light curves from active galaxies **2003**, *MNRAS*, 345, 1271
23. Bhatta, G., & Webb, J. Microvariability in BL Lacertae: "Zooming" into the Innermost Blazar Regions, *Galaxies*, **2018**, 6, 2
24. Leahy, D. A., Elsner, R. F., & Weisskopf, M. C. On searches for periodic pulsed emission - The Rayleigh test compared to epoch folding *ApJ* **1983**, 272, 256
25. Davies, S. R. An improved test for periodicity *MNRAS*, **1990**, 244, 93
26. Davies, S. R. Davies Periodicity Test Revisited *MNRAS*, **1991**, 251, 64P
27. Zhang, B.-K., Zhao, X.-Y., Wang, C.-X., & Dai, B.-Z. Optical quasi-periodic oscillation and color behavior of blazar PKS 2155-304 *RAA*, **2014**, 14, 933-941
28. Larsson, S. Parameter estimation in epoch folding analysis, *A&AS*, **1996**, 117, 197
29. Lomb, N. R. Least-squares frequency analysis of unequally spaced data, *Ap&SS*, **1976**, 39, 447

30. Scargle, J. D. Studies in astronomical time series analysis. II - Statistical aspects of spectral analysis of unevenly spaced data *ApJ*, **1982**, 263, 835
31. VanderPlas, J. T. Understanding the Lomb–Scargle Periodogram **2018**, *ApJS*, 236, 16
32. Edelson, R. A., & Krolik, J. H. The discrete correlation function - A new method for analyzing unevenly sampled variability data, *ApJ*, **1988** 333, 646
33. Villata, M., Raiteri, C. M., Aller, H. D., et al. The WEBT campaigns on BL Lacertae. Time and cross-correlation analysis of optical and radio light curves 1968-2003 **2004**, *A&A*, 424, 497
34. Press, W. H. Flicker noises in astronomy and elsewhere *Comments on Astrophysics*, **1978**, 7, 103
35. Uttley, P., McHardy, I. M., & Papadakis, I. E. Measuring the broad-band power spectra of active galactic nuclei with RXTE *MNRAS*, **2002**, 332, 231
36. Timmer, J., & Koenig, M. On generating power law noise *A&A* **1995**, 300, 707
37. Valtonen, M. J., Lehto, H. J., Takalo, L. O., et al. Testing the 1995 binary black hole model of OJ287 *ApJ*, **2011**, 729, 33–38
38. Komossa, S. Observational evidence for binary black holes and active double nuclei *MmSA* **2006**, 77, 733
39. Peters, P. C. Gravitational Radiation and the Motion of Two Point Masses *Physical Review*, **1964**, 136, 1224
40. Kharb, P., Lal, D. V., & Merritt, D. A candidate sub-parsec binary black hole in the Seyfert galaxy NGC 7674 *Nature Astronomy*, **2017**, 1, 727
41. Ackermann, M., Ajello, M., Albert, A., et al. Multiwavelength Evidence for Quasi-periodic Modulation in the Gamma-Ray Blazar PG 1553+113 *ApJL*, **2015**, 813, L41
42. Camenzind, M., & Krockenberger, M. The lighthouse effect of relativistic jets in blazars - A geometric origin of intraday variability *A&A* **1992**, 255, 59
43. Mohan, P., & Mangalam, A. Kinematics of and Emission from Helically Orbiting Blobs in a Relativistic Magnetized Jet *ApJ*, **2015**, 805, 91
44. Rieger, F. M. Supermassive binary black holes among cosmic gamma-ray sources *Ap&SS* **2007**, 309, 271
45. Stella, L., & Vietri, M. Lense-Thirring Precession and Quasi-periodic Oscillations in Low-Mass X-Ray Binaries *ApJL*, **1998**, 492, L59
46. Motta, S., Muñoz-Darias, T., Casella, P., Belloni, T., & Homan, J. Low-frequency oscillations in black holes: a spectral-timing approach to the case of GX 339-4 *MNRAS*, **2011**, 418, 2292
47. Liska, M., Hesp, C., Tchekhovskoy, A., et al. Formation of precessing jets by tilted black hole discs in 3D general relativistic MHD simulations *MNRAS*, **2018**, 474, L81
48. Graham, M. J., Djorgovski, S. G., Stern, D., et al. A systematic search for close supermassive black hole binaries in the Catalina Real-time Transient Survey *MNRAS*, **2015**, 453, 1562
49. Li, L.-X., & Narayan, R. Quasi-periodic Oscillations from Rayleigh-Taylor and Kelvin-Helmholtz Instability at a Disk-Magnetosphere Interface *ApJ*, **2004**, 601, 414
50. Fu, W., & Lai, D. Dynamics of the innermost accretion flows around compact objects: magnetosphere-disc interface, global oscillations and instabilities *MNRAS*, **2012**, 423, 831
51. McKinney, J. C., Tchekhovskoy, A., & Blandford, R. D. *MNRAS*, **2012**, 423, 3083

Sample Availability: Samples of the compounds ..... are available from the authors.